ISSN 1087-6596, Glass Physics and Chemistry, 2017, Vol. 43, No. 4, pp. 368–375. © Pleiades Publishing, Ltd., 2017.
Original Russian Text © N.Yu. Koval'ko, M.V. Kalinina, A.N. Malkova, S.A. Lermontov, L.V. Morozova, I.G. Polyakova, O.A. Shilova, 2017, published in Fizika i Khimiya Stekla.

Synthesis and Comparative Studies of Xerogels, Aerogels, and Powders Based on the ZrO_2–Y_2O_3–CeO_2 System

N. Yu. Koval'ko[a, *], M. V. Kalinina[a], A. N. Malkova[b], S. A. Lermontov[b], L. V. Morozova[a], I. G. Polyakova[a], and O. A. Shilova[a, c]

[a] *Grebenshchikov Institute of Silicate Chemistry, Russian Academy of Sciences, St. Petersburg, 199034 Russia*
[b] *Institute of Physiologically Active Substances, Russian Academy of Sciences, Chernogolovka, Moscow oblast, 142432 Russia*
[c] *Ul'yanov (Lenin) St. Petersburg State Electrotechnical University LETI, St. Petersburg, 197022 Russia*
**e-mail: kovalko.n.yu@gmail.com*

Received December 29, 2016

Abstract—The technology of liquid-phase synthesis of mesoporous xerogels and aerogels based on ZrO_2–Y_2O_3–CeO_2 is developed. Xerogels are obtained by the coprecipitation of hydroxides, while aerogels are obtained in accordance with the sol–gel technology: the average pore size is 1.5–17.2 nm and the specific surface area is 120–878 m^2/g. Aerogels are characterized by a high degree of porosity: the pore volume attains 1–4 cm^3/g. Based on precursor xerogels, nanopowders of a tetragonal solid solution of the $(ZrO_2)_{0.92}(Y_2O_3)_{0.03}(CeO_2)_{0.05}$ composition with a particle size of 5–9 nm and S_{spec} = 74 m^2/g were fabricated. Due to the high values of their specific surface area, the synthesized xerogels and aerogels are promising as sorbents, catalysts, or catalyst supports.

Keywords: zirconium dioxide, xerogels, aerogels, hydroxide coprecipitation, sol–gel technology, mesoporosity, physical–chemical properties

DOI: 10.1134/S108765961704006X

INTRODUCTION

Recently, the interest in studies of materials with particle size not exceeding a few nanometers has been constantly increasing due to the core differences of their properties from those of micro-sized powders and materials based on them [1, 2]. The unique electric, mechanical, magnetic, optic, and other properties of nanomaterials are responsible for their application in various fields of medicine, power and mechanical engineering, etc.

Among numerous ceramic materials, the most promising in terms of application are those based on zirconium dioxide partially stabilized with oxides of rare-earth elements in cubic and tetragonal structures. Materials of this type are characterized with a wide range of physical–chemical properties: chemical and thermal stability, mechanical strength, hardness, strong resistance to cracking, low heat conductivity, high ionic electroconductivity, etc. Transition to nanosized structures allows increasing the values of the specific surface area and adsorption capacity, as well as improving the materials' chemical reactivity and catalytic properties. However, creating the technologies for the production of materials on the basis of nanopowders is impossible without reliable data on their morphological, size, and structural characteristics. Thus, studying the primary products of the synthesis of ceramic materials (xerogels and aerogels) constitutes a necessary task, as the very stage of xerogel formation is the one, during which the structure and size of the grains of ceramics on its basis are formed. Aerogels are produced by the sol–gel method with subsequent supercritical drying of alcogels, namely, the removal of the solvent from pores of the gel at temperatures exceeding the critical temperature [3–8].

Nanodispersed xerogels and aerogels based on zirconium dioxide are wide applied as superlight construction materials and modifying additives to them, heterogeneous catalysts, and catalyst supports [9–11]. To produce low-agglomeration xerogels, aerogels, and highly dispersed powders on their basis, different methods of liquid-phase synthesis are used: combined hydroxide coprecipitation, sol–gel method, etc. [12, 13].

The objective of the present work consisted in the synthesis of xerogels, aerogels, and powders in the ZrO_2–Y_2O_3–CeO_2 system by different liquid-phase methods (coprecipitation and sol–gel method) and the study of their physical–chemical properties.

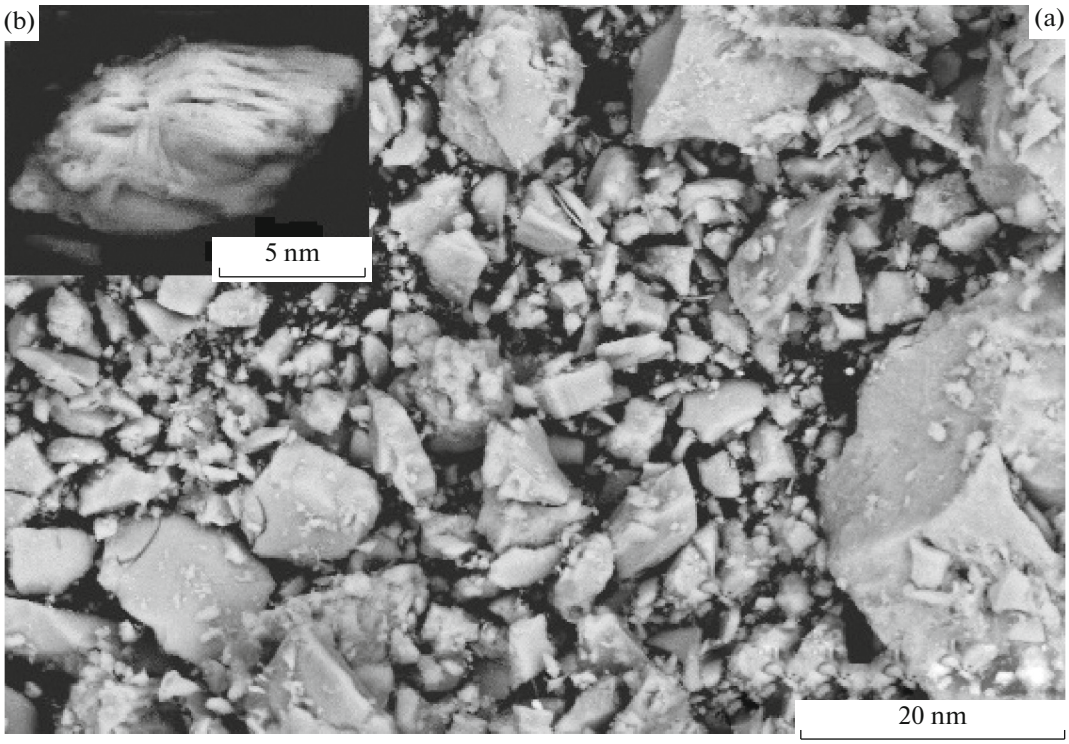

Fig. 1. Microstructure of xerogel of the $(ZrO_2)_{0.92}(Y_2O_3)_{0.03}(CeO_2)_{0.05}$ composition fabricated by method of hydroxide coprecipitation.

EXPERIMENTAL

Study methods. The following study methods were used in the present work. The pH of hydroxide precipitation was determined by the pH measurement method (150 M pH-meter). The powders specific surface area and pore size distribution were determined by the method of low-temperature nitrogen adsorption (gas sorption analyzer Autosorb-1 and Quantachrome Nova 4200e). The differential thermal analysis (DTA) was used to study the processes occurring in coprecipitated xerogels, aerogels, and powders on heating in the temperature range 20–1000°C (Q-1000 derivatograph, MOM). The powders' phase composition was determined by the method of X-ray diffraction analysis (XRD) (D8 Advance Bruker diffractometer, CuK_α radiation, $2\theta = 15°–80°$ in air). The X-ray images were refined using an international ICDD-2006 database. The coherent scattering region (CSR) was calculated using the PDWin software package developed by NPO Burevestnik. The ceramics' microstructure was determined by the method of scanning electron microscopy using an NVision 40 working station (Carl Zeiss). The powders' IR transmission spectra were obtained using a Vertex 70 Fourier transform IR spectrometer (Bruker).

Synthesis of xerogels and aerogels based on the ZrO_2–Y_2O_3–CeO_2 system and tetragonal solid solution of the composition $(ZrO_2)_{0.92}(Y_2O_3)_{0.03}(CeO_2)_{0.05}$. Synthesis of xerogels and powders by the method of coprecipitation in the system was carried out from solutions of zirconium, yttrium, and cerium nitrates by aqueous ammonia solution using the cryochemical treatment (freezing at –25°C). The following concentrations of the initial aqueous solutions were selected: 0.1 M $ZrO(NO_3)_2 \cdot 2H_2O$, 0.1 M $Y(NO_3)_3 \cdot 5H_2O$, 0.1 M $Ce(NO_3)_3 \cdot 6H_2O$, and 1 M NH_4OH. Precipitation was carried out at pH 9–10. Upon completion of the precipitation process, the time that the precipitate was left in the solution was minimized to avoid the processes of olation and oxolation, characteristic of zirconium hydroxide and that result in the formation of polymer compounds [12, 14–16]. According to the XRD data, the obtained xerogels are X-ray amorphous with particle sizes in the range 5–8 nm and consist of fine granules of rounded shapes with a low degree of agglomeration of ~30–40 nm (Figs. 1, 2).

The thermal treatment of amorphous precursors at 400°C results in the crystallization of the solid solution based on zirconium hydroxide in a metastable cubic structure of the fluorite (c-ZrO_2) with the average crystallite size of ~6 nm (Fig. 2). The temperature increase up to 600°C yields the formation of a tetragonal solid solution based on ZrO_2; the average size of the t-ZrO_2 crystallites is 11 nm.

Aerogel samples in the ZrO_2–Y_2O_3–CeO_2 system were synthesized by the sol–gel technology. The zir-

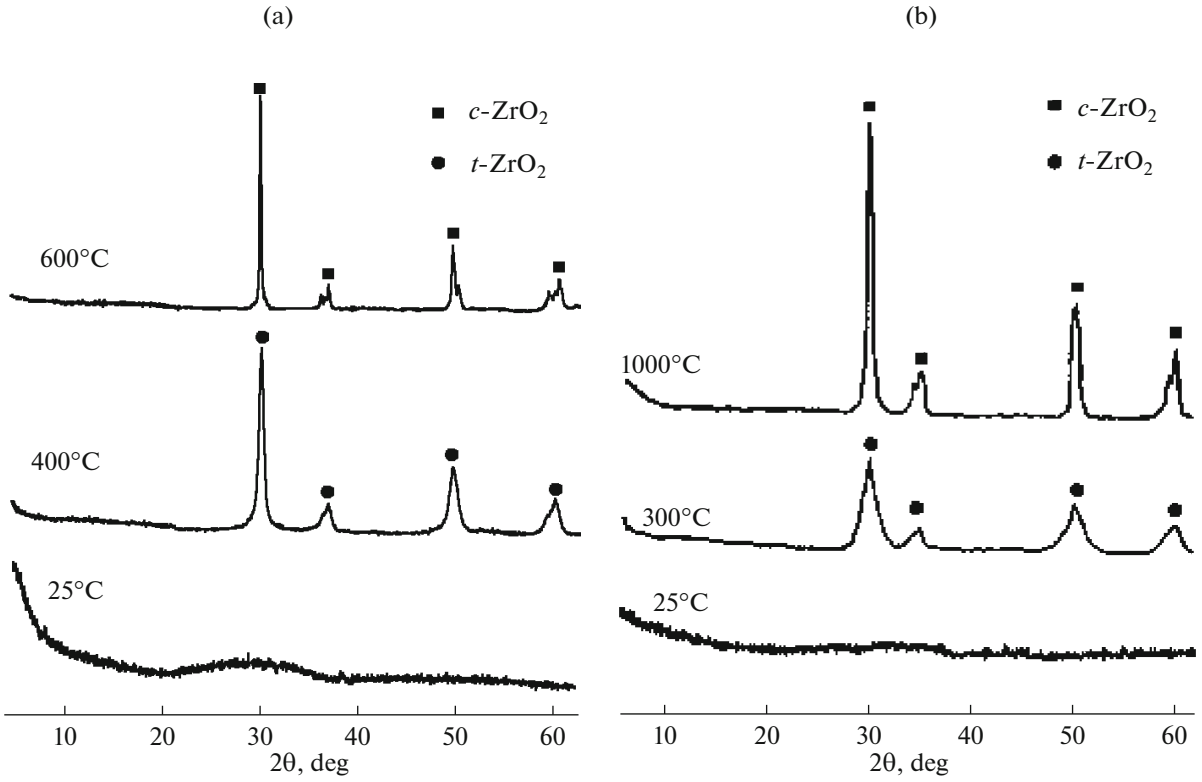

Fig. 2. Sequence of process of formation of t-ZrO_2 phase in samples of xerogel fabricated by method of coprecipitation (a) and aerogel dried in MTBE (b).

conium oxynitrate powder was dissolved in methanol and, thereafter, cerium and yttrium nitrates, as well as a catalyst for gel formation (propylene oxide), were added. The gels were formed within 20–30 min, held at room temperature for 24 h, and then washed by different solvents once a day for 7 days in order to replace the liquid in the pores by pure solvent [7, 17].

Isopropyl alcohol (IPA), methyltert-butyl ether (MTBE), and carbon dioxide (CO_2) were selected as the solvents. Heating was carried out in an autoclave until the temperature exceeded the solvent's critical temperature, and then the mixture was held at this temperature for 10–15 min. For IPA and MTBE, the drying temperatures were 250–260°C (6.0–7.0 MPa) and 235–245°C (6.0–7.0 MPa), respectively. During supercritical drying in carbon dioxide, the sample was washed with liquid CO_2 (20°C, 15 MPa). Then, the temperature in the reactor was increased to 50°C, and the sample was washed by supercritical CO_2 (15 MPa) [17]. Thus, aerogel samples in the ZrO_2–Y_2O_3–CeO_2 system dried in IPA, MTBE, and carbon dioxide were fabricated.

RESULTS AND DISCUSSION

The behavior of the synthesized samples of xerogels and aerogels of the $(ZrO_2)_{0.92}(Y_2O_3)_{0.03}(CeO_2)_{0.05}$ composition on heating was investigated by the differential thermal analysis (Figs. 3, 4). Figure 3 shows the DTA/TG curves for xerogels synthesized by the method of coprecipitation of zirconium, yttrium and cerium hydroxides with elements of cryotechnology. We observe the endo-effect corresponding to the main stage of precipitate dehydration with the mass loss of about 10% in the range 110–150°C. Such an insignificant mass loss is related to the fact that freezing the coprecipitated gels decreases the quantity of water in the crystal hydrates of amorphous hydroxides, which is related to the increase of the dispersity of the precipitated powder and the start of the dehydration process as early as during the drying of the hydroxide precipitate [12, 13]. The narrow exo-effect around 435°C indicates the explosive character of the crystallization yielding a cubic solid solution of $(ZrO_2)_{0.92}(Y_2O_3)_{0.03}(CeO_2)_{0.05}$ (c-ZrO_2) with the average particle size of 5–8 nm, which is in agreement with the XRD results. The further temperature increase up to 600°C results in the formation of the nanostructured single-phase tetragonal solid solution (t-ZrO_2, 10–12 nm).

Figures 4a–4c show the DTA and TG curves for different aerogel samples. All the DTA curves (Figs. 4a–4c) contain overlapping peaks of the exothermal effects in the temperature ranges 210–290°C and 280–350°C, indicating the occurrence of the pro-

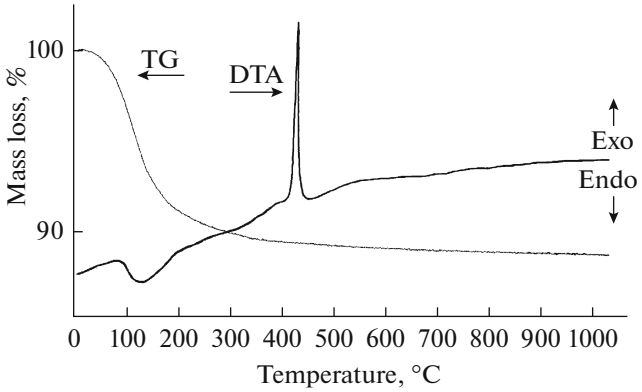

Fig. 3. Results of differential thermal analysis of xerogel fabricated by method of hydroxide coprecipitation with cryo-treatment.

cesses of burning-out of the excess CH groups and carbon and the start of crystallization of the metastable cubic structure (c-ZrO_2). These processes occur with mass losses of 30–40% depending on the aerogel drying method.

The studies of the characteristics of the texture of the fabricated samples were carried out by the method of the low-temperature adsorption of nitrogen (Fig. 5). Figures 5a and 5b show the adsorption–desorption isotherms and the pore size distribution curves for xerogel and powder of the $(ZrO_2)_{0.92}(Y_2O_3)_{0.03}(CeO_2)_{0.05}$ composition synthesized by the coprecipitation method.

As seen from Fig. 5a, the capillary–condensation hysteresis is not expressed clearly, whereas the sorption curve type indicates the microporous structure of the xerogel (type I of the IUPAC classification) [19]. The characteristic appearance of the sorption curve for the nanopowder (Fig. 5b) enables us to confirm its mesoporous structure (type V of the IUPAC classification), while the type of the capillary–condensation hysteresis reveals the presence of bottle-like mesopores. As seen from the figure, in the xerogel sample (a), micropores (~2 nm) are predominant, the total pore volume is 0.136 cm^3/g, and the specific surface area is 120.4 m^2/g. In the nanodispersed powder sample (b), the number of micropores is significantly smaller, while the number of fine mesopores increased (~5–7 nm). The total pore volume was 0.129 cm^3/g.

As an example, Fig. 5c shows the isotherm of nitrogen adsorption–desorption on the $(ZrO_2)_{0.92}$-$(Y_2O_3)_{0.03}(CeO_2)_{0.05}$ sample synthesized by the sol–gel method and dried in the MTBE. As seen from Fig. 5c, the type of the sorption curve allows us to speak of the mesoporous structure of the aerogel (type III of the IUPAC classification), whereas the type of the capillary–condensation enables us to state the presence of pores of a slit-like shape of a diameter of ~22 nm. The specific surface area was 495 m^2/g. The aerogel is characterized with a wide pore size distribution ranging from 1 to 120 nm. The characteristics of the porous structure of the aerogels dried in other media (isopropyl alcohol and carbon dioxide) are presented in Table 1. We can see that the largest values of the specific surface area

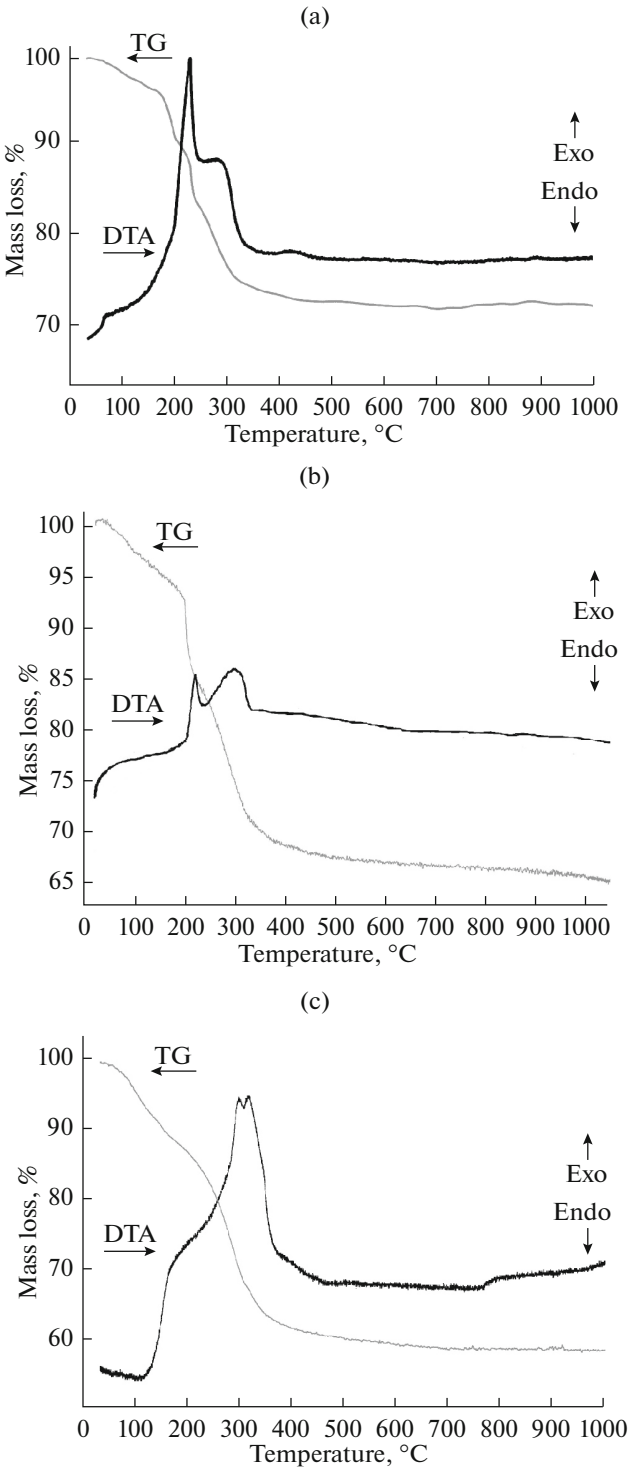

Fig. 4. Results of differential thermal analysis of aerogel fabricated in accordance with sol–gel technology dried in IPA (a), MTBE (b), and CO_2 (c).

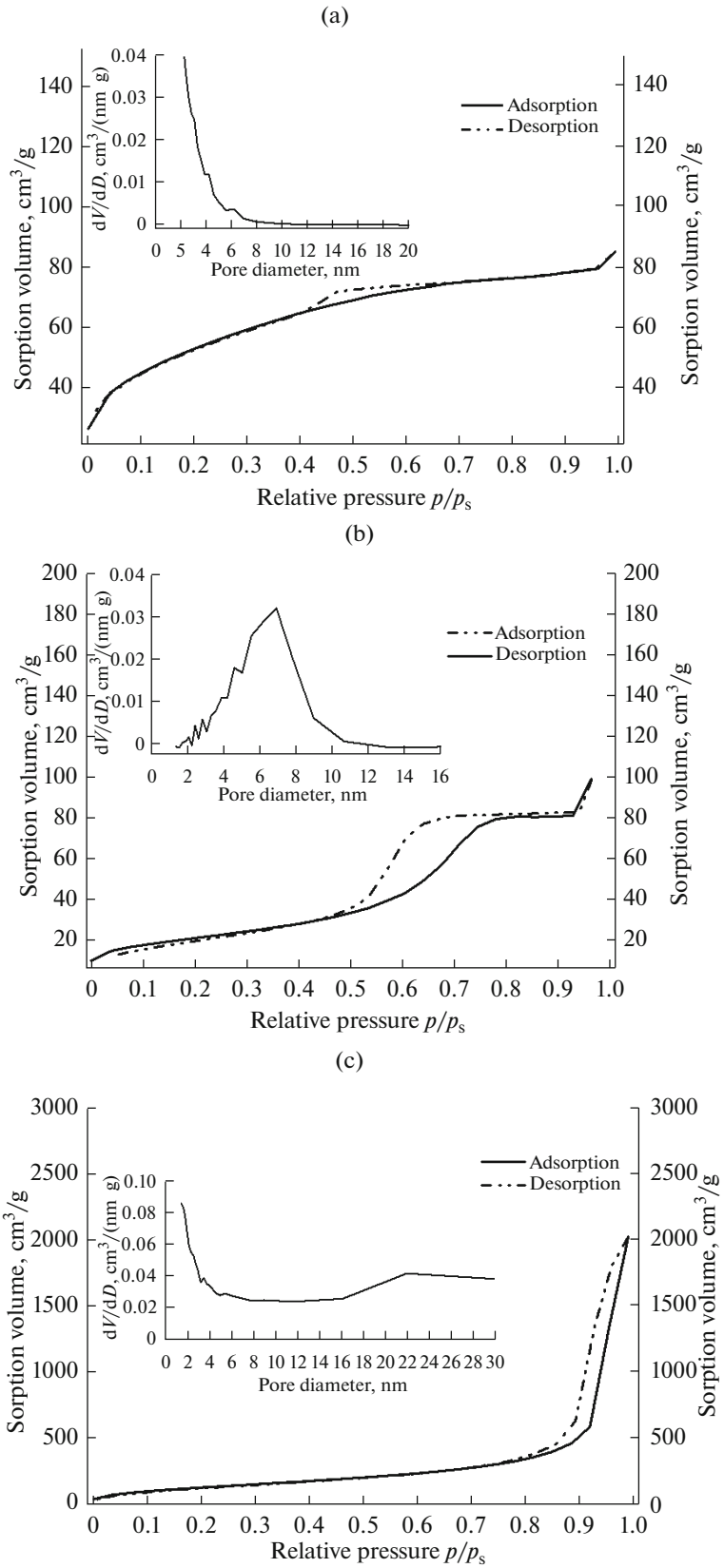

Fig. 5. Isotherms of adsorption–desorption and differential curves of pore size distribution for xerogel synthesized by method of coprecipitation (a), nanopowder of the $(ZrO_2)_{0.92}(Y_2O_3)_{0.03}(CeO_2)0.05$ composition upon thermal treatment at 600 °C (b), and aerogel of the $(ZrO_2)_{0.92}(Y_2O_3)_{0.03}(CeO_2)_{0.05}$ composition synthesized by sol–gel method and dried in MTBE (c).

Table 1. Characteristics of porous structure of xerogels, aerogels, and powders of the $(ZrO_2)_{0.92}(Y_2O_3)_{0.03}(CeO_2)_{0.05}$ composition

Method of synthesis	Conditions of synthesis	Phase composition	Specific surface area, S_{spec}, m^2/g	Sorption volume, V_s, m^3/g	Total pore volume, cm^3/g	Average pore volume, nm	Average particle size, d, nm
Coprecipitation	T_{form} = 25°C	Amorphous	120.4	85.7	0.121	1.33	2.9*
	T_{form} = 400°C	*c*-phase	84.1	101.1	0.090	5.16	5.5*; 8.7**
	T_{form} = 600°C	*t*-phase	64.1	90.2	0.073	12.5	10.1**
Sol–gel	Drying in IPA T_{form} = 25°C	Amorphous	878.5	2524.6	4.058	1.07	9.7*
	Drying in MTBE T_{form} = 25°C	Amorphous	815.5	2022.4	3.265	1.08	9.9*
	Drying in CO_2, T_{form} = 25°C	Amorphous	436.1	1058.0	1.674	17.17	11.6*

* Calculations of average particle size were performed in accordance with Gurvich formula: $d = 4V_s/S_{spec}$ [18]; ** according to CSA.

Table 2. Results of X-ray diffraction analysis of samples of aerogels fabricated in different solvents (IPA, MTBE, CO_2) upon thermal treatment at different temperatures

T_{form}, °C	Sample					
	aerogel dried in IPA		aerogel dried in MTBE		aerogel dried in CO_2	
	phase, crystal lattice parameters	CSA, nm	phase, crystal lattice parameters	CSA, nm	phase, crystal lattice parameters	CSA, nm
25	Amorphous, crystallization start	–	Amorphous	–	Amorphous	–
300	Metastable cubic a = 5.108 Å	13	Metastable cubic a = 5.119 Å	68	Amorphous	–
1000	Tetragonal a = 3.623 Å c = 5.191 Å	25	Tetragonal a = 3.626 Å c = 5.194 Å	73	Tetragonal a = 3.625 Å c = 5.193 Å	35

(878 m^2/g) and total mesopore volume (4 cm^3/g) characterize the aerogels dried in isopropyl alcohol, which is determined by the properties of the solvent that is of primary importance in the aerogel synthesis. The phase composition of aerogels obtained in different solvents can also be different. For example, the X-ray image of the aerogel based on ZrO_2 fabricated by drying in isopropyl alcohol contains reflections around 30°, characteristic of a metastable crystalline cubic structure, while an amorphous aerogel is formed when drying in ether (Fig. 2b). The formation of a crystalline cubic structure in the case of the sample obtained using isopropyl alcohol must be related to the fact that the critical parameters of this solvent and, therefore, the temperature of supercritical drying of this aerogel significantly exceed the similar values for MTBE and CO_2.

The sizes of particles of aerogels obtained through drying in different solvents and under different thermal treatment and the parameters of crystal structures are shown in Table 2. The phase composition of aerogels determined by the XRD method is in good agreement with the data obtained by the method of scanning electron microscopy (Figs. 6a–6c). As seen from Fig. 6, the aerogels fabricated using different solvents have complex micromorphologies characterized with a homogeneous framework of the porous structure.

Xerogels are characterized with the values S_{spec} = 120 m^2/g and total pore volume 0.13 cm^3/g, which are substantially smaller than the respective parameters for aerogels: S_{spec} = 440–878 m^2/g and 2–4 cm^3/g, respectively. Such differences are related to the fact that the aerogel framework remains unchanged under supercritical drying (just the solvent is removed), while xerogels shrink and aggregate upon thermal treatment, which affects their characteristics, especially the values of specific surface areas [4–6, 20].

The synthesized xerogels, aerogels, and powders were investigated by the method of Fourier transform IR spectroscopy (Fig. 7). The IR spectra of all the samples contain a wide area of diffuse absorption in

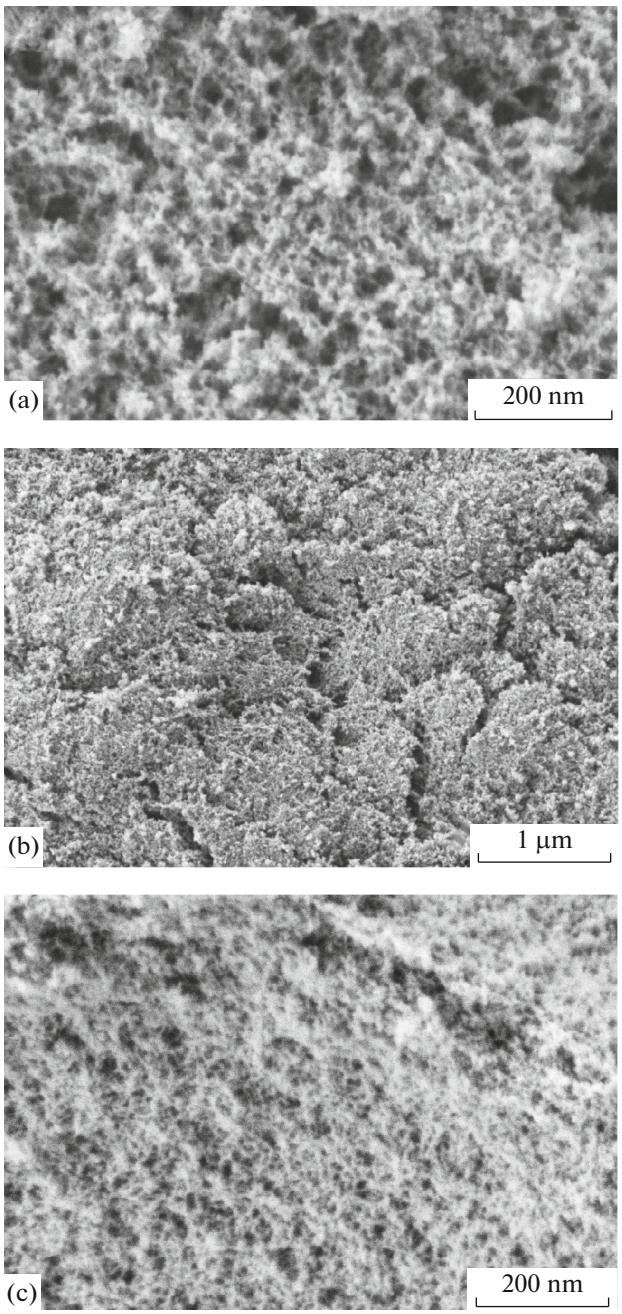

Fig. 6. Microstructure of aerogels of the $(ZrO_2)_{0.92}$-$(Y_2O_3)_{0.03}(CeO_2)_{0.05}$ composition fabricated in accordance with the sol–gel technology dried in isopropyl alcohol (IPA) (a), methyltert-butyl ether (MTBE) (b), and carbon dioxide CO_2 (c).

the range 400–800 cm^{-1}, indicating the presence of Zr–O and O–Zr–O oxygen bridges. On curve *1*, the set of absorption bands around 1380 and 1550 cm^{-1} assumes the presence of a water "bridge" coordinated by two zirconium ions on the surface of the ZrO_2-based xerogel: Zr^{4+}–H_2O–Zr^{4+}.

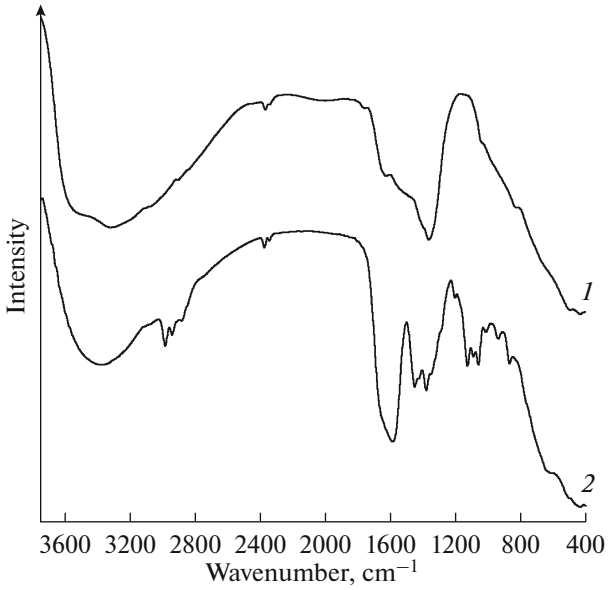

Fig. 7. IR spectrum of xerogel of $(ZrO_2)_{0.92}$-$(Y_2O_3)_{0.03}(CeO_2)_{0.05}$ composition fabricated by method of coprecipitation (*1*) and aerogel fabricated in accordance with sol–gel technology dried in methyltert-butyl ether (MTBE) (*2*).

The bands around 1280, 1310, and 1420 cm^{-1}, characterizing vibrations of CH and CH_2 groups are observed on curve *2*. Besides, the peaks in the 2800–3000 cm^{-1} range characterizing the stretching vibrations of the unhydrated CH_3 and CH_2 groups are present on the same curve.

The presence of these groups is caused by using MTBE during the synthesis of the aerogel sample. The characteristic feature of curve *2* consists in the presence of Zr–OH–Zr bonds (800–900 cm^{-1}) and crystallization water (1600–1650 cm^{-1}). Probably, the existence of these bonds and the bound water is determined by the sample fabrication methods, in particular, the sol–gel technology and aerogel drying at supercritical temperatures.

All the curves are characterized by the presence of a broad absorption band around 3400 cm^{-1}, corresponding to the stretching vibrations of the adsorbed water determined by the liquid-phase synthesis methods used in fabricating the samples under study.

CONCLUSIONS

The suggested technologies of synthesis, coprecipitation and the sol–gel method, allow us to obtain mesoporous xerogels with a particle size of 5–8 nm and a low degree of agglomeration (~30–40 nm) and aerogels with a particle size of 9–10 nm. The thermolysis and the textural and structural features of the fabricated xerogels, aerogels, and powders in the ZrO_2–Y_2O_3–CeO_2 system have been investigated. The synthesized

precursors manifest single phase areas of the existence of cubic and tetragonal solid solutions in the temperature range 300–1000°C. Due to the significant specific surface area and, as a result, the large number of active surface sites, xerogels and aerogels are applied as superlight construction materials, sorbents, highly efficient heterogenous catalysts, and catalyst supports.

ACKNOWLEDGMENTS

The aerogel synthesis was financially supported by the Russian Science Foundation (project no. 14-13-01150).

REFERENCES

1. *Nanotekhnologii* (Nanotechnology) Tret'yakov, Yu.D., Eds., Moscow: Fizmatlit, 2009.
2. Alymov, M.I., *Poroshkovaya metallurgiya nanokristallicheskikh materialov* (Powder Metallurgy of Nanocrystalline Materials), Moscow: Nauka, 2007.
3. Shishmakov, A.B., Koryakova, O.V., Mikushina, Yu.V., and Petrov, L.A., Synthesis and comparative analysis of porous binary oxides ZrO_2-SiO_2 synthesized based on zirconium(IV) and tetrabutoxyzirconium using cellulose as a matrix, *Khim. Rastit. Syr'ya,* 2015, no. 3, pp. 151—159.
4. *Aerogels Handbook,* Aegerter, M.A., Leventis, N., and Koebel, M.M., Heidelberg: Springer, 2011.
5. Rao, A.V., Hegde, N.D., and Hirashima, H., *J. Colloid Interface Sci.,* 2007, vol. 305, p. 124.
6. Lermontov, S.A., Sipyagina, N.A., Malkova, A.N., Baranchikov, A.E., and Ivanov, V.K., Effect of synthetic conditions on the properties of methyltrimethoxysilane-based aerogels, *Russ. J. Inorg. Chem.,* 2014, vol. 59, no. 12, pp. 1392—1395.
7. Lermontov, S.A., Sipyagina, N.A., Malkova, A.N., Baranchikov, A.E., Sidorov, A.A., Efimov, N.N., Ugolkova, E.A., Minin, V.V., Ivanov, V.K., and Eremenko, I.L., New aerogels chemically modified with amino complexes of bivalent copper, *Russ. J. Inorg. Chem.,* 2015, vol. 60, no. 12, pp. 1459–1463.
8. Lermontov, S.A., Sipyagina, N.A., Malkova, A.N., Baranchikov, A.E., Erov, Kh.E., Petukhov, D.I., and Ivanov, V.K., Methyltrimethoxysilane-based elastic aerogels: effects of the supercritical medium on structure-sensitive properties, *Russ. J. Inorg. Chem.,* 2015, vol. 60, no. 4, pp. 488–493.
9. Iler, R.K., *The Chemistry of Silica: Solubility, Polymerization, Colloid and Surface Properties and Biochemistry of Silica,* New York: Wiley, 1979, pt. 2.
10. Gusev, A.I., *Nanomaterialy, nanostruktury, nanotekhnologii* (Nanomaterials, Nanostructures, Nanotechnologies), Moscow: Nauka-Fizmatlit, 2007.
11. Manankov, A.V., Physicochemical principles of nanostructural mineralogy in modern materials production, *Vestn. TGASU,* 2012, no. 2, pp. 120–136.
12. Morozova, L.V., Kalinina, M.V., Koval'ko, N.Yu., and Drozdova, I.A., Synthesis and study of nanocompositions based on zirconia dioxide for new biomaterials creation, *Fiz. Khim. Stekla,* 2012, vol. 38, no. 6, pp. 946–950.
13. Morozova, L.V., Kalinina, M.V., Koval'ko, N.Yu., Arsent'ev, M.Yu., and Shilova, O.A., Preparation of zirconia-based nanoceramics with a high degree of tetragonality, *Glass Phys. Chem.,* 2014, vol. 40, no. 3, pp. 352–355.
14. Panova, T.I., Morozova, L.V., and Polyakova, I.G., Synthesis and investigation of properties of nanocrystalline dioxides zirconia and hafnia, *Glass Phys. Chem.,* 2011, vol. 37, no. 2, pp. 179–187.
15. Sato, T. and Shimada, M., Control of the tetragonal-to-monoclinic phase transformation of yttria partially stabilized zirconia in hot water, *J. Mater. Sci.,* 1985, vol. 2, pp. 3988–3992.
16. Tret'yakov, Yu.D., Oleinikov, N.N., and Mozhaev, A.P., *Osnovy kriokhimicheskoi tekhnologii* (The Basic Principles of Cryochemical Technology), Moscow: Vysshaya Shkola, 1987.
17. Yorov, Kh.E., Sipyagina, N.A., Malkova, A.N., Baranchikov, A.E., Lermontov, S.A., Borilo, L.P., and Ivanov, V.K., Methyl tert-butyl ether as a new solvent for the preparation of SiO_2–TiO_2 binary aerogels, *Inorg. Mater.,* 2016, vol. 52, no. 2, pp. 163–169.
18. Dudarko, O.A. and Zub, Yu.L., Studying the structure of phosphoryl xerogels by transmission electron microscopy, *Sorbtsion. Khromatogr. Protsessy,* 2014, vol. 14, no. 6, pp. 895–901.
19. Gregg, S. and Sing, K., *Adsorption, Surface Area and Porosity,* London: Academic, 1982.
20. Dubinin, M.M., *Adsorbtsiya i poristost'* (Adsorption and Porosity), Moscow: Izd. VAKhZ, 1972.

Translated by D. Marinin